Interaction of Two Prolamins with 1-^{13}C Oleic Acid by ^{13}C NMR†

L. A. Forato,‡ V. E. Yushmanov,§ and L. A. Colnago*,‡

Embrapa Instrumentação Agropecuária, Rua XV de Novembro 1452, São Carlos-SP, 13560-970, Brazil, Department of Anesthesiology, University of Pittsburgh, Pittsburgh, Pennsylvania 15213

Received September 1, 2003; Revised Manuscript Received February 20, 2004

ABSTRACT: In this paper, we analyzed the interaction of Z19 prolamin from a BR451 maize variety and pennisetin from a BRS1501 pearl millet variety with 1-^{13}C-enriched oleic acid (OA) by ^{13}C NMR in solution. In both proteins, we identified the presence of free fatty acids by NMR in solid state and solution. The interactions were analyzed at the protein/OA molar ratios of 1:1 and 1:4. In the Z19/OA 1:1 mixture in 70% ethanol and 30% D_2O, the chemical shift of OA C1 was 182.9 ppm, about 3 ppm above that of the pure OA in the same solvent. In contrast, upon addition of OA to the pennisetin (1:1), the chemical-shift value slightly decreased by less than 1 ppm. The chemical-shift titration curve of OA C1 in an apparent pH range of 5.5−7.3 shifted by approximately 0.3 pH units toward higher pH values in the pennisetin/OA 1:1 complex relative to the pure OA. The results obtained for the pennisetin/OA 1:4 mixture were similar to the complexes at a 1:1 molar ratio. A significant difference was observed between the 1:1 and 1:4 curves for Z19. The titration curve for Z19/OA 1:1 suggested specific binding at the sites with electrostatic interaction.

Zeins, the main maize storage proteins, have been extensively studied because of their nutritional and industrial applications (*1*, *2*). Zeins are classified into α, *β*, *γ*, and *δ* zeins according to their solubility and are deposited in organelles known as protein bodies located in the maize endosperm (*3*, *4*). The α zeins represent more than 70% of the total zeins present in maize and are characterized by the presence of two protein fractions in sodium dodecyl sulfate−polyacrilamide gel electrophoresis (SDS−PAGE)[1], Z19 and Z22, with molecular masses of 19 and 22 kDa, respectively (*2*, *4*). They contain nonrepeatable domains at the C and N termini and homologous repeats in the central region (*5*). They are insoluble in water and soluble in 70% ethanol, where they show significant α-helical content, up to 60% as measured by circular dichroism and Fourier transform infrared spectroscopy (*4*−*7*). Recently, we have demonstrated that α zeins extracted by 70% ethanol have a similar proportion of secondary structures to the ones purified without contact with an organic solvent, indicating that this solvent does not increase the helical content as observed in others proteins (*8*).

We have recently identified the presence of free fatty acids in α zeins and protein bodies using ^{1}H and ^{13}C nuclear magnetic resonance (NMR) (*9*). This finding justified the comparison of the fatty-acid-binding properties of α zeins to those of other proteins from plant and animal tissues that are able to bind fatty acids. For this purpose, endogenous fatty acids were extracted from the nonseparated mixture of α zeins, and preliminary results on the interaction of α zeins with 1-^{13}C-enriched oleic acid (OA) were obtained by ^{13}C NMR. It was shown that the interaction involves electrostatic and hydrophobic components (*10*). The purpose of the present work was to analyze the fatty acid interaction with two purified prolamins, the Z19 fraction from maize cultivar (BR451) and pennistin from pearl millet (BRS1501), similar to maize Z22 prolamin (*10*−*12*). The study of the binding of OA with these proteins by ^{13}C NMR indicates that Z19 has ionic interactions with this fatty acid, whereas the interaction of pennisetin with OA is possibly dominated by the hydrophobic forces.

EXPERIMENTAL PROCEDURES

Sample Preparation. 1-^{13}C-OA (99.9% enrichment), deuterated DMSO-d_6, and ethanol-d_6 were from Cambridge Isotope Laboratories (Andover, MA), and deuterated water (D_2O) was from Isotec (Miamisburg, OH). Water, whenever used, was deionized (Milli-Q, Millipore, Bedford, MA). Ethanol (C_2H_5OH), chloroform ($CHCl_3$), sodium acetate (CH_3COONa), sodium phosphate (Na_2HPO_4), and sodium chloride (NaCl) of a reagent or analytical grade were obtained from commercial sources.

The fraction of Z19 from BR451 maize cultivar grains and pennisetin from BRS1501 pearl millet cultivar were obtained as described elsewhere (*9*). First, apolar lipids were removed from the cereal grains by hexane extraction for 24 h in a söxlet apparatus. After that, the proteins were extracted with 70% ethanol and lyophilized, and their purity was characterized by SDS−PAGE. After the solid-state ^{13}C and ^{1}H NMR experiments, the remaining endogenous free fatty acids were removed by chloroform (*9*). The lipids extracted

† This work was supported by grants from Brazilian agencies, CNPq 301274/01-0; FAPESP, 97/13449-1; and Embrapa, 12.0.98.816.

* To whom correspondence should be addressed. E-mail: colnago@cnpdia.embrapa.br. Phone: 55-16-274-2477. Fax: 55-16-272-5958.

‡ Embrapa de Novembro 1452.

§ University of Pittsburgh.

[1] Abbreviations: NMR, nuclear magnetic resonance; OA, oleic acid; SDS−PAGE, sodium dodecyl sulfate−polyacrilamide gel electrophoresis; GC−MS, gas chromatography/mass spectrometry; CPMAS, cross polarization with magic-angle spinning; MAS, magic-angle spinning; BSA, bovine serum albumin; FABP, fatty-acid-binding protein; LTP, lipid-transfer protein.

10.1021/bi035562k CCC: $27.50
Published on Web 05/12/2004

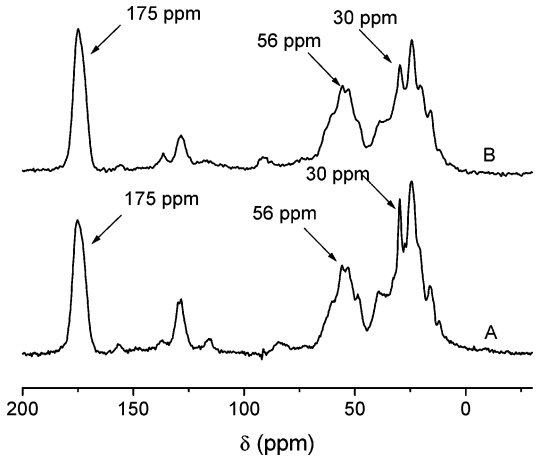

FIGURE 1: High-resolution solid-state ^{13}C CPMAS NMR spectra of the Z19 (A) and pennistein (B) proteins.

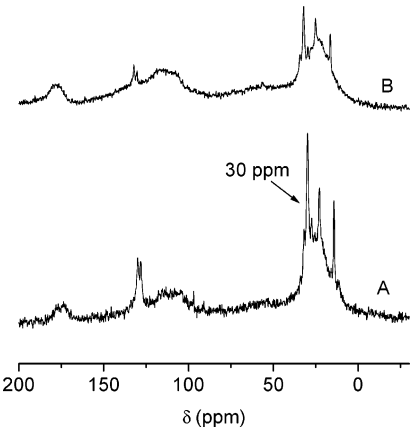

FIGURE 2: Single-pulse MAS solid-state ^{13}C NMR spectra of Z19 (A) and pennisetin (B).

by chloroform were analyzed by gas chromatography/mass spectrometry (GC−MS) and ^1H and ^{13}C NMR. GC−MS was performed on the lipid extracts on an HP-5890 chromatograph coupled to a mass detector HP-5970 using a column of 50-m length and 0.22-mm diameter with a 0.33-μm film thickness. For ^1H NMR analysis, the proteins were solubilized in DMSO-d_6. For ^{13}C NMR spectroscopy of the protein/OA complexes, the solvent mixture contained either 70% absolute ethanol and 30% D_2O by volume, or 70% absolute ethanol, 27% 30 mmol/L phosphate buffer, and 3% D_2O. The pH values of the phosphate buffer (herein referred to as apparent pH) in these preparations varied from 5.5 to 7.3 in 0.25 steps. OA was added to 1 mmol/L protein solutions to the desirable final protein/OA molar ratio between 1:1 and 1:16.

NMR Analysis. NMR measurements were performed on a Varian Unity INOVA 400 spectrometer with a magnetic field of 9.4 T at 30 °C, if not stated otherwise. For ^{13}C NMR experiments in solution, the spectral width was 25 kHz, the acquisition time was 1.2 s, the recycle time was 2.5 s, and the pulse width was $\pi/2$. The postprocessing exponential filter with a line-broadening factor of 5 Hz was applied in the time domain. The ^1H NMR solution-state spectra of Z19 and pennisetin were recorded in DMSO-d_6 at 30 °C using 32 scans, a $\pi/2$ pulse, and a 3-s repetition time.

For solid-state ^{13}C NMR measurements, the cross polarization technique with magic-angle sample spinning (CP-MAS) was used. The lyophilized protein samples were packed into zirconium rotors and spun at 9 kHz. The spectra were acquired into 2048 data points using the pulse width of $\pi/2$, contact time of 1 ms, recycle time of 3 s, decoupling bandwidth of 60 kHz, spectral width of 40 kHz, and 3000 scans. All spectra were filtered by an exponential decay function (line-broadening factor of 20 Hz). In addition, Z19 and pennisetin were analyzed using single-pulse excitation, i.e., the simplest pulse sequence consisting of only a single pulse, with magic-angle spinning (MAS) (*13*). The recycle time was 3 s, and the number of scans was 10 000.

RESULTS

NMR Characterization of Z19 and Pennisetin. The solid-state CPMAS spectra of Z19 and pennisetin samples prior to the chloroform extraction are presented in Figure 1. They show signals at 175 ppm, from 100 to 160 ppm, from 70 to 45 ppm, and between 45 and 15 ppm, which are the typical signals of the protein carbons of the carbonyl groups, aromatic side chains, α carbons, and aliphatic side chains, respectively. A strong peak at 30 ppm, more intense in Z19 than in the pennisetin spectrum, is not typical of the proteins, being rather characteristic of hydrocarbon chains. To confirm the presence of lipids, we applied the single-pulse MAS technique, which is useful to detect the substances with relatively high mobility and short T_1 in a solid sample (*9*, *13*). This technique detects only lipids rather than proteins. Figure 2 shows the absence of characteristic glycerol backbone peaks at 62 and 69 ppm in the single-pulse MAS solid-state ^{13}C NMR spectra of Z19 and pennisetin, suggesting that the signal originates from fatty acids rather than triglycerides.

To confirm the presence of free fatty acids, the lipids extracted by chloroform were analyzed by GC−MS and by solution-state ^1H and ^{13}C NMR. The GC−MS analysis has shown myristic, palmitic, stearic, oleic, and linoleic acids as the main extract components. The ^1H and ^{13}C NMR spectra of extracted lipids were typical of free fatty acids, lacking the glycerol backbone resonances, and showed a high content of unsaturated fatty acids (oleic and linoleic acids), similar to the earlier findings in lipids extracted from the fraction of the total α zeins and from protein bodies of corn grains (*9*). The endogenous free fatty acids represent 5 and 1% of the mass of purified Z19 and pennisetin proteins, respectively, as measured by chloroform extraction. The higher content of free fatty acids in Z19 than in the pennisetin samples was confirmed by the high-intensity signals at 5.3 and 1.2 ppm in ^1H NMR spectra in solution (Figure 3).

The broad signal at 172 ppm (Figure 2), assigned to the carboxyl groups of free fatty acids (*9*) is an indication of its lower mobility in comparison with other carbons in the chain and its putative interaction with proteins. To confirm this hypothesis, we analyzed the interaction of 1-^{13}C-enriched OA in 70% ethanol by ^{13}C NMR.

Interaction of Z19 and Pennisetin with 1-^{13}C OA. Because the presence of free fatty acids in Z19 and pennisetin proteins was confirmed, similar to the recent findings in the total α zeins (*9*), an attempt was made to gain insight into the mechanism of interaction of these two prolamins with fatty acids. To this end, the endogenous fatty acids were extracted from the protein samples by chloroform, and the interaction of Z19 and pennisetin with exogenous OA was studied by ^{13}C

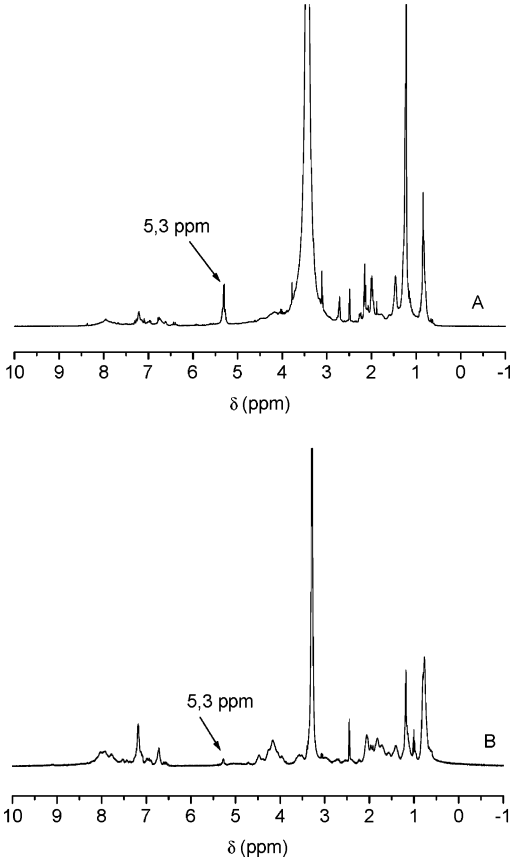

FIGURE 3: ^{1}H NMR spectrum of Z19 (A) and pennisetin (B) in DMSO-d_6 at 30 °C. Residual DMSO signal appears at 2.49 ppm.

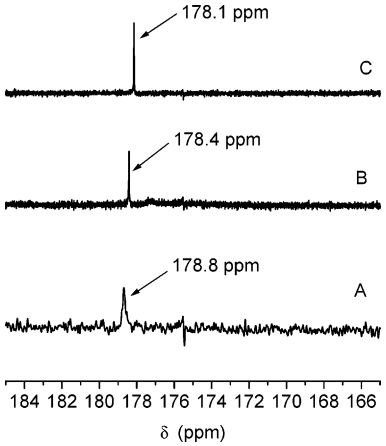

FIGURE 4: Expanded carboxyl region of ^{13}C NMR spectra of 1-^{13}C-enriched OA in the pennisetin/OA complexes in 70% ethanol and 30% D_2O. (A) Pure OA, (B) pennisetin/OA 1:1, and (C) pennisetin/OA 1:16. The spectra were recorded at 30 °C.

NMR in solution. A single peak of the carboxyl C1 carbon, whose chemical shift depended on the particular sample conditions, was observed in the OA complexes with both Z19 and pennisetin, as well as with the total α zeins (*10*).

Figure 4 shows an expanded carboxyl region in the ^{13}C NMR spectra of 1 mmol/L 1-^{13}C-enriched pure OA in 70% ethanol and 30% D_2O and of OA in the presence of pennisetin in the same solvent at molar ratios of pennisetin/OA of 1:1 and 1:16. In the pure OA, this signal appeared at 178.8 ppm, whereas it was slightly displaced upfield to approximately 178 ppm when pennisetin was added at pennisetin/OA molar ratios of 1:1 and 1:16.

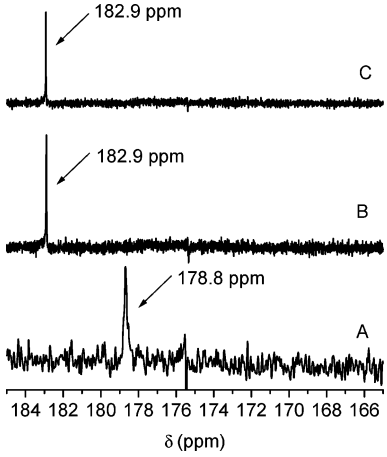

FIGURE 5: Expanded carboxyl region of ^{13}C NMR spectra of 1-^{13}C-enriched OA in the Z19/OA complexes in 70% ethanol and 30% D_2O. (A) Pure OA, (B) Z19/OA 1:1, and (C) Z19/OA 1:16. The spectra were recorded at 30 °C.

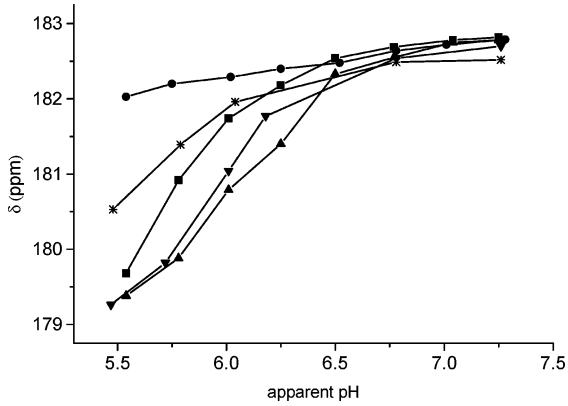

FIGURE 6: Titration curves of the ^{13}C NMR chemical shift of the carboxyl C1 carbon in 1 mM 1-^{13}C-enriched OA (■), the 1:1 complexes pennisetin/OA (▲) and Z19/OA (●), and the 1:4 complexes pennisetin/OA (▼) and Z19/OA (*). Apparent pH states for the pH value of the phosphate buffer in the solvent mixture containing 70% absolute ethanol, 27% 30 mmol/L phosphate buffer, and 3% D_2O.

^{13}C NMR spectra of 1 mmol/L pure OA in 70% ethanol and 30% D_2O and of OA in the presence of Z19 are presented in Figure 5. In contrast to pennisetin, the addition of Z19 at the molar ratio of protein/OA of 1:1 and 1:16 resulted in the chemical shift increase of the carboxyl carbon of OA to 182.9 ppm.

To obtain more detailed information about the mechanism of interaction of the pennisetin and Z19 with OA, the chemical shift of the carboxyl ^{13}C of OA was monitored in the presence of the two proteins. To maintain apparent pH in the range of 5.5−7.3 [the same range as for the other fatty-acid-binding proteins (*14*)], the solutions were prepared in the mixture of 70% absolute ethanol, 27% 30 mmol/L phosphate buffer, and 3% D_2O. Shown in Figure 6 are the titration curves of the complexes pennisetin/OA and Z19/OA and of OA without adding protein. The molar ratios of prolamin/OA were 1:1 and 1:4. At pH 7 and above, the C1 chemical shift (182.8 ppm) was independent of the presence of the protein. At pH below 7 in the presence of pennisetin, the observed chemical shift was lower than that of the pure OA; i.e., the whole titration curve displaced to the right, which is equivalent to a moderate increase in the apparent

p*K* of OA. In contrast, in the presence of Z19, the chemical shift was higher than that of the pure OA. The peak position did not experience significant changes over the whole pH range at 1:1 Z19/OA molar ratio. At the 4:1 excess of OA over prolamins, the titration curves occupied positions intermediate between those of the pure OA and a corresponding 1:1 complex, seemingly because both the tightly bound OA and the excess of OA contributed to the signal. In the titration curves of the total α zeins/OA complex, no significant difference from the pure OA was found (data not shown).

DISCUSSION

The mechanisms of fatty acid interactions with Z19 and pennisetin were studied using ^{13}C NMR methodology that was successfully applied earlier to bovine serum albumin (BSA), which has several binding sites for OA, and to intracellular fatty-acid-binding proteins (FABPs) (*15*−*17*). For BSA, the authors observed several carboxyl signals at different concentrations of protein/OA, corresponding to different types of binding sites (*16*). In contrast, a single carboxyl peak, whose position varied with the OA concentration in protein/OA complexes, appeared in the present study. This finding may be interpreted as the fast (on a NMR time scale) exchange of OA between binding sites on the proteins and solution, so that only the averaged signal results. Fast exchange may be due to the extended linear structure of zein and pennisetin proteins (*11*, *18*), with fatty-acid-binding sites exposed to the solvent. Among FABPs that bind more than one molecule of a long-chain fatty acid, a single carboxyl signal for OA was observed previously in liver FABP (*15*), and rapid exchange of at least one of the bound OA with the bulk oleate pool has been suggested (*17*).

We proposed earlier that putative fatty-acid-binding sites on α zeins involve only arginine residues, because lysines are absent from these proteins (*9*). This basic amino acid is a carrier of the positive charge on the zein surface, and its guanidinum group could attract the ionized carboxylic groups of the fatty acids. Indeed, most known α-zein sequences contain one to three arginines (*2*, *19*). In particular, the sequences of Z19 and Z22 (which is similar to pennisetin) have three arginine residues per molecule, and the positions of two of them are highly conserved among the α-zein family (*9*). Therefore, our initial assumption was that the fatty-acid-binding sites on Z19 and pennisetin are likely to include the arginine residues.

Indeed, in the Z19/OA mixture, the chemical shift of OA C1 was 182.9 ppm, about 3 ppm above that of the pure OA (Figure 5). This indicates that the OA binding to Z19 occurs at polar, probably ionizable, sites. Interaction with positively charged arginines would favor dissociation of the OA carboxyl group and a downfield shift of the carboxyl carbon peak (*16*). Pennisetin, however, showed an opposite trend. Upon addition of OA to the protein, the chemical-shift value slightly decreased by less than 1 ppm (Figure 4). This indicates that the carboxyl group of OA becomes more shielded, that is, the ionized form of the carboxyl group is not favored in the presence of pennisetin and that the hydrophobic interactions between the carbonic chain of OA and the nonpolar amino acid side chains contribute significantly to the mechanism of interaction of OA with pennisetin.

Titration curves of the chemical shift of OA C1 with and without adding protein were obtained in an apparent pH range of 5.5−7.3 (Figure 6). In this pH range, the chemical shift of OA C1 varied from 179.4 to 182.8 ppm. The whole titration curve for the pennisetin/OA complex shifted toward higher apparent pH values relative to the pure OA. In contrast, the C1 chemical shift in the Z19/OA titration varied from 182.0 to 182.8 ppm, i.e., almost 3 ppm above that of pure OA at pH 5.5. These results confirm that dissociation of the carboxyl proton is facilitated in the presence of Z19. It is well-known that displacements of ionization equilibria in the system of interacting ionic species result in changes in the apparent p*K* values of the species involved (*20*, *21*). Accordingly, the titration curve for Z19/OA may be interpreted as a strong decrease in the apparent p*K* of OA upon its interaction with Z19. Similar behavior was reported for the rat intestinal FABP in the complex with palmitic acid (*22*). Titration data in Figure 6 support our hypothesis that Z19 has an electrostatic interaction with the carboxyl group of OA, resulting in its ionization. The positive charges on the protein surface are likely to originate from the guanidinum group of the arginine residues; two of the three arginines are in conserved positions in Z19 (*9*). We observed a significant difference between the 1:1 and 1:4 curves for Z19. This indicates that Z19 has only a limited number (one or two) of specific binding sites with electrostatic interaction (which are characterized by a significant p*K* displacement to the lower values), whereas the excess of OA molecules find themselves in an apolar environment, either in the protein or in the solvent. In the case of pennisetin, however, this protein showed a predominantly hydrophobic interaction with OA, resulting in the lower values of the chemical shift of the carboxyl carbon in the presence of pennisetin.

These results underscore that binding of fatty acids to prolamins occurs through the intricate network of ionic and hydrophobic interactions at their binding sites. Despite the fact that these proteins contain conserved arginines and both are supposedly linear with binding sites exposed to the solvent (*18*), their interaction with OA is determined mainly by electrostatic forces for Z19 and is mainly hydrophobic for pennisetin. In other proteins with the ability to bind fatty acids, different combinations of ionic and hydrophobic forces are also responsible for a great variability of fatty-acid-binding sites. Plant lipid-transfer proteins (LTP), found in maize (*23*−*25*) and other cereals and possibly participating in the movement of fatty acids and other lipids between membranes, are small (7 and 9 kDa) basic mainly α-helical proteins. The binding of fatty acids to maize LTPs has been characterized by X-ray crystallography, NMR, and fluorescent labeling (*23*, *24*, *26*−*30*). It was shown that most of the fatty acid acyl chain is buried inside the hydrophobic cavity and the polar head interacts with the charged side chains at one of the ends of the cavity (*27*, *28*). The presence of a hydrogen bond between the hydroxyl of Tyr81 and the carbonyl of the lipid was reported (*23*). The possible involvement of the H4 helix (*26*) and four disulfide bonds (*24*) in the lipid-binding site and importance of lipid−lipid interactions in the binding process (*29*) were suggested. Maize LTP shows preferential binding of C16 to C19 fatty acids and a total binding capacity of two lipids with different affinity (*24*, *29*, *30*). The two different conformations of bound OA, the structural plasticity of the ligand-binding

cavity, and the predominance of the van der Waals interactions with the hydrocarbon chain of the fatty acid have been demonstrated (*30*). It has been further shown that the modes of binding and orientation of the palmitate in the maize and barley LTPs are different, although no conformational changes occur in either of the proteins upon fatty acid binding (*31*).

When different functionally related proteins were compared, it was suggested that some of the myristate-binding sites in human serum albumin resemble those in the maize LTP, implying the role of α-helical domains in the nonspecific binding of fatty acids (*30*). The presence of two types of binding sites, which either do or do not form ion pairs with fatty acids, has been suggested earlier for BSA (*32*). Plant LTPs share a lack of specificity and a similar mode of action with structurally unrelated animal FABPs, where a delicate balance of ionic and hydrophobic forces also determines the binding of fatty acids. In a recent NMR structural study of the invertebrate FABP, a network of hydrogen bonds of the water scaffold was postulated inside the ligand-binding cavity, created by polar side chains in the center section and a cluster of hydrophobic residues at the bottom of the cavity (*33*). In the rat intestinal FABP, the NMR structure and ^{15}N relaxation-derived backbone dynamics showed that a single molecule of fatty acid is trapped inside the cavity protected from the bulk solvent (*34*). In the liver FABP, two OA molecules bound within its cavity (*17*, *35*) and the total solubilization capacity of up to 8 equiv of OA (*17*) were suggested based on X-ray and NMR data. The hydrogen-bonding network within the cavity was shown to include the carboxyl OA group and the side chains of arginine and serine residues, whereas the carboxyl moiety of another OA lies near the FABP surface and is exposed to the solvent (*35*).

Although the high-resolution structure of the zein complex with fatty acids is currently unavailable, the difference in the mechanism of OA binding to Z19 and pennisetin leads us to hypothesize that the network of ionic and hydrophobic interactions and hydrogen bonds may be significantly different for these two proteins. The arginines may be shielded, or the hydrophobic sites are overwhelming or more attractive for OA on pennisetin as compared to those (i.e., sites) on Z19.

REFERENCES

1. Rothfus, J. A. (1996) Potential β-sheet surfaces of corn and wheat proteins, *J. Agric. Food Chem. 44*, 3143−3152.
2. Lasztity, R. (1996) *The Chemistry of Cereal Proteins*, 2nd ed., CRC Press, New York, NY.
3. Colnago, L. A., and Forato, L. A. (2002) in *Advanced Studies in Agricultural Instrumentation* (Cruvinel, P. E., and Mascarenhas, S., Eds.) pp 89−98, RIMA Editora, São Carlos, Brazil.
4. Shewry, P. R., and Tatham, A. S. (1990) The prolamin storage proteins of cereal seeds: Structure and evolution, *Biochem. J. 267*, 1−12.
5. Argos, P., Pedersen, K., Marks, M. D., and Larkins, B. A. (1982) A structural model for maize zein proteins, *J. Biol. Chem. 257*, 9984−9990.
6. Wu, Y. V., Paulis, J. W., Sexson, K. R., and Wall, J. S. (1983) Conformation of corn zein and glutelin fractions with unusual amino acid sequence, *Cereal Chem. 50*, 342−344.
7. Krestchmer, B. (1957) Infrared spectroscopy and optical rotatory dispersion of zein, wheat, and gliadin, *J. Phys. Chem. 61*, 1627−1631.
8. Forato, L. A., Bicudo, T. C., and Colnago, L. A. (2003) Conformation of α zeins in solid state by FTIR, *Biopolymers 72*, 421−426.
9. Forato, L. A., Colnago, L. A., Garratt, R. C., and Lopes, M. A. (2000) Identification of free fatty acids in maize protein bodies and purified α zeins by ^{13}C and ^{1}H nuclear magnetic resonance, *Biochim. Biophys. Acta 1543*, 106−114.
10. Forato, L. A., Yushmanov, V. E., and Colnago, L. A. (2000) in *VI Jornada Brasileira de Ressonância Magnética*, pp 133−134, Belo Horizonte, MG, Brazil.
11. Forato, L. A., Doriguetto, A. C., Fischer, H., Masarenhas, Y. P., Craievich, A. F., and Colnago, L. A. (2004) Conformation of the Z19 Prolamin by FTIR, NMR, and SAXS, *J. Agric. Food Chem. 52*, 2382−2385.
12. Sainani, M. N., Mishra, V. K., Gupta, V. S., and Ranjekar, P. K. (1992) Circular dichroism and ^{13}C nuclear magnetic resonance spectroscopy of pennisetin from pearl millet, *Plant Sci. 83*, 15−22.
13. Rutar, V. (1989) Magic angle sample spinning NMR spectroscopy of liquids as a nondestructive method for studies of plant seeds, *J. Agric. Food Chem. 37*, 67−70.
14. Beringhelli, T., Goldoni, L., Capaldi, S., Bossi, A., Perduca, M., and Monaco, H. L. (2001) Interaction of chicken liver basic fatty acid-binding protein with fatty acids: a ^{13}C NMR and fluorescence study, *Biochemistry 40*, 12604−12611.
15. Cistola, D. P., Walsh, M. T., Corey, R. P., Hamilton, J. A., and Brecher, P. (1988) Interactions of oleic acid with liver fatty acid binding protein: a carbon-13 NMR study, *Biochemistry 27*, 711−717.
16. Hamilton, J. A. (1991) in *Carbon-13 NMR Spectroscopy of Biological Systems*, pp 117−157, Academic Press, San Diego, CA.
17. Wang, H., He, Y., Kroenke, C. D., Kodukula, S., Storch, J., Palmer, A. G., and Stark, R. E. (2002) Titration and exchange studies of liver fatty acid-binding protein with ^{13}C-labeled long-chain fatty acids, *Biochemistry 41*, 5453−5461.
18. Bugs, M. R., Forato, L. A., Bortoletto-Bugs, R. K., Fischer, H., Mascarenhas, Y. P., Ward, R. J., and Colnago, L. A. (2004) Spectroscopic characterization and structural modelling of prolamin from pearl millet (*Pennisetum americanum*), *Eur. Biophys. J. 33*, 335−343.
19. Tatham, A. S., Shewry, P. R., and Belton, P. S. (1990) in *Advanced Cereal Technology* (Pomeranz, Y., Ed.) pp 1−78, American Association of Cereal Chemists, St. Paul, MN.
20. Rabenstein, D. L., Bratt, P., Schierling, T., Robert, J. M., and Guo, W. (1992) The interaction of biological molecules with heparin and related glycosaminoglycans. I. Identification of a specific heparin binding site for histamine, *J. Am. Chem. Soc. 114*, 3278−3285.
21. Yushmanov, V. E., Perussi, J. R., Imasato, H., Ruggiero, A. C., and Tabak, M. (1994) Ionization and binding equilibria of papaverine in ionic micelles studied by ^{1}H NMR and optical absorption spectroscopy, *Biophys. Chem. 52*, 157−163.
22. Cistola, D. P., Sacchettini, J. C., Banaszak, L. J., Walsh, M. T., and Gordon, J. I. (1989) Fatty acid interactions with rat intestinal and liver fatty acid-binding proteins expressed in *Escherichia coli*. A comparative ^{13}C NMR study, *J. Biol. Chem. 264*, 2700−2710.
23. Gomar, J., Sodano, P., Sy, D., Shin, D. H., Lee, J. Y., Suh, S. W., Marion, D., Vovelle, F., and Ptak, M. (1998) Comparison of solution and crystal structures of maize nonspecific lipid transfer protein: a model for a potential in vivo lipid carrier protein, *Proteins 31*, 160−171.
24. Zachowski, A., Guerbette, F., Grosbois, M., Jolliot-Croquin, A., and Kader, J. C. (1998) Characterisation of acyl binding by a plant lipid-transfer protein, *Eur. J. Biochem. 257*, 443−448.
25. Castro, M. S., Gerhardt, I. R., Orru, S., Pucci, P., and Bloch, C., Jr. (2003) Purification and characterization of a small (7.3 kDa) putative lipid transfer protein from maize seeds, *J. Chromatogr., B 794*, 109−114.
26. Petit, M. C., Sodano, P., Marion, D., and Ptak, M. (1994) Two-dimensional ^{1}H NMR studies of maize lipid-transfer protein. Sequence-specific assignment and secondary structure, *Eur. J. Biochem. 222*, 1047−1054.
27. Shin, D. H., Lee, J. Y., Hwang, K. Y., Kim, K. K., and Suh, S. W. (1995) High-resolution crystal structure of the nonspecific lipid-transfer protein from maize seedlings, *Structure 3*, 189−199.
28. Gomar, J., Petit, M. C., Sodano, P., Sy, D., Marion, D., Kader, J. C., Vovelle, F., and Ptak, M. (1996) Solution structure and lipid

binding of a nonspecific lipid transfer protein extracted from maize seeds, *Protein Sci. 5*, 565−577.
29. Douliez, J., Michon, T., and Marion, D. (2000) Steady-state tyrosine fluorescence to study the lipid-binding properties of a wheat nonspecific lipid-transfer protein (nsLTP1), *Biochim. Biophys. Acta 1467*, 65−72.
30. Han, G. W., Lee, J. Y., Song, H. K., Chang, C., Min, K., Moon, J., Shin, D. H., Kopka, M. L., Sawaya, M. R., Yuan, H. S., Kim, T. D., Choe, J., Lim, D., Moon, H. J., and Suh, S. W. (2001) Structural basis of non-specific lipid binding in maize lipid-transfer protein complexes revealed by high-resolution X-ray crystallography, *J. Mol. Biol. 308*, 263−278.
31. Lerche, M. H., and Poulsen, F. M. (1998) Solution structure of barley lipid transfer protein complexed with palmitate. Two different binding modes of palmitate in the homologous maize and barley nonspecific lipid transfer proteins, *Protein Sci. 7*, 2490−2498.
32. Cistola, D. P. (1998) Fat sites found! *Nat. Struct. Biol. 5*, 751−753.
33. Lücke, C., Kizilbash, N., Van Moerkerk, H. T., Veerkamp, J. H., and Hamilton, J. A. (2003) NMR assignment and structural characterization of the fatty acid binding protein from the flight muscle of *Locusta migratoria*, *J. Biomol. NMR 25*, 355−356.
34. Hodsdon, M. E., and Cistola, D. P. (1997) Ligand binding alters the backbone mobility of intestinal fatty acid-binding protein as monitored by ^{15}N NMR relaxation and ^{1}H exchange, *Biochemistry 36*, 2278−2290.
35. Thompson, J., Winter, N., Terwey, D., Bratt, J., and Banaszak, L. (1997) The crystal structure of the liver fatty acid-binding protein. A complex with two bound oleates, *J. Biol. Chem. 272*, 7140−7150.

BI035562K